High Power Laser Science and Engineering, (2014), Vol. 2, e41, 12 pages.

doi:10.1017/hpl.2014.46

Optimization of relativistic laser–ion acceleration

J. Schreiber[1,2], F. Bell[1], and Z. Najmudin[3]

[1]*Fakultät für Physik, Ludwig-Maximilians-Universität München, Am Coulombwall 1, D-85748 Garching, Germany*

[2]*Max-Planck-Institut für Quantenoptik, Hans-Kopfermann-Str. 1, D-85748 Garching, Germany*

[3]*The John Adams Institute, Blackett Laboratory, Imperial College London, London SW7 2AZ, United Kingdom*

(Received 4 September 2014; revised 30 October 2014; accepted 11 November 2014)

Abstract

Experiments have shown that the ion energy obtained by laser–ion acceleration can be optimized by choosing either the appropriate pulse duration or the appropriate target thickness. We demonstrate that this behavior can be described either by the target normal sheath acceleration model of Schreiber *et al.* or by the radiation pressure acceleration model of Bulanov and coworkers. The starting point of our considerations is that the essential property of a laser system for ion acceleration is its pulse energy and not its intensity. Maybe surprisingly we show that higher ion energies can be reached with reduced intensities.

Keywords: laser–ion acceleration; relativistic laser plasma interaction

1. Introduction

Laser-driven ion acceleration has created enormous interest over the last few years[1, 2]. The rapid development of laser technology to intensities well beyond 10^{20} W cm^{-2} has enabled the generation of multi-MeV ion beams with exceptional characteristics[3]. Visions of reaching electron energies in the TeV[4] and even the PeV regime[5] have been published. While the ion beams in most experiments have exhibited extremely broad energy distributions, advanced target designs have been applied to achieve narrow energy distributions of protons and heavier ions[6–9]. The early, rapid developments have engendered much speculation about the use of laser-driven ions for fast ignition[10–12] and medical applications[13–17]. Laser-generated protons have already been successfully applied for time-resolved studies of the generation of electric and magnetic fields in the laser–plasma interaction on a ps timescale[18–20]. Moreover, the table-top generation of neutrons is discussed as a possible application and has been demonstrated in early and recent experiments[21–25].

The observation of ions emitted in laser–plasma interactions can first be traced to experiments employing high-intensity laser pulses with durations of a few ns to some hundreds of ps[26]. With the invention of chirped pulse amplification (CPA)[27], laser pulses with intensities well in excess of 10^{18} W cm^{-2} and fs durations were realized. The new era of relativistic laser–plasma interactions had begun, where the quiver velocity of electrons in the electromagnetic field of the laser approaches the speed of light. Moreover, the $v \times B$-term of the Lorentz force becomes dominant and pushes the electrons into the direction of laser propagation. The generation of relativistic electrons was the fundamental requisite for the acceleration of ions to high energy[28]. Foils of several tens of micrometer thickness which were irradiated by relativistically intense laser pulses were found to emit protons with energies of up to 60 MeV from the non-irradiated surface[29]. This behavior could be described by the target normal sheath acceleration (TNSA)[30] which has proved to be the dominant mechanism in most experiments performed until recent times. In recent years, competing mechanisms for ion acceleration have been introduced and discussed, the most prominent example being the radiation pressure acceleration (RPA)[31–40] or light-sail regime[41–44] which utilizes highly intense laser pulses with high contrast. Not too differently from the original ideas on the forces due to radiation[45–50], it seems feasible to accelerate the central part of an ultra-thin, nm scale foil to high energies according to the simple equation of motion[51].

Although a number of high-power, PW-class laser systems have been built around the world, the early record energy of 60 MeV[29] has improved little. Supported by analytical models, we demonstrate that this is due to the optimization

Correspondence to: J. Schreiber, Fakultät für Physik, Ludwig-Maximilians-Universität München, Am Coulombwall 1, D-85748 Garching, Germany. Email: Joerg.Schreiber@lmu.de

problem that is encountered in both TNSA and RPA. We show that the key quantity of a laser system is its energy content in a single laser pulse. The laser energy simply is converted with a certain efficiency into a number and energy of ions and it is not the intensity that is most important as often intuitively assumed. This statement holds for both TNSA and RPA. As we will show, TNSA can be optimized by varying, even increasing, the duration of the laser pulse (i.e., decreasing intensity) and RPA by choosing an optimized target thickness. Although reduction of the pulse duration for a laser system of given energy means an increase in power and intensity, this also reduces the acceleration time so that inertial ions cannot reach the same final energy.

2. Target normal sheath acceleration

TNSA of ions has been extensively investigated over the last decade. In fact, until now it has proved to be the most effective method for ion acceleration when highly intense laser pulses are focused onto foils with thicknesses of several micrometers. TNSA relies on the efficient conversion of laser energy into hot, relativistic electrons. These electrons propagate through the target and set up fields at the target boundaries where they exit into vacuum. The electric field is created between the expelled electrons and the surface charge that they induce on the target. Since the electric field strength is of the same relative strength as the laser electric field amplitude (TV/m) which generates the hot electrons, most of the electrons return back into the target. Hence an electron cloud (sheath) is formed. Ions at the rear surface can be accelerated by the sheath fields to multi-MeV energies in only several tens of femtoseconds. Impurities such as hydrocarbon and water are present under most experimental conditions at the solid surface. Due to their higher charge-to-mass ratio, it is the protons from these contaminants that are most readily accelerated to high energies. However, by removing the contaminants by different means, the acceleration of heavier ions can also be optimized[52–55]. Due to strong spatial and temporal variations in the acceleration fields, the observed ions usually exhibit broad energy distributions extending from zero to a certain maximum cut-off energy. Reduction of this energy spread is a major challenge and some success has been achieved by micro-machining the targets in order to allow ions to be accelerated only in regions where the field is large and roughly uniform[6, 7], and by the use of mass-limited targets with an appropriate ion mixture[8, 56].

A large number of experimental results on laser-driven ion acceleration are now available[7, 29, 57–70], which can be used for a comparison with theoretical predictions. TNSA has been extensively studied numerically using particle-in-cell (PIC) simulations[71–75]. Several analytical models have also been developed which predict the dependence of the maximum ion energy on laser and target parameters[57, 76–82]. Substantial advance of the field is reported in a number of review papers available today[1, 2, 83]. In particular, the ion energy should be dependent on the laser irradiance, focal spot size and laser pulse duration.

2.1. Nonrelativistic TNSA

The original Schreiber model[57] is a nonrelativistic version of TNSA and calculates the energy gain of ions in an electrostatic field determined by the transfer of laser energy to the expanding surface by the divergent beam of hot electrons. This model has two main advantages. (i) Without choosing a distribution function for the laser-accelerated electrons, the potential that they set up depends only on the absorbed laser power ηP_L into those electrons and the transverse size of the electron cloud R_s. (ii) Due to the consideration of the transverse dimension R_s of the electron cloud when it exits the rear of the target, the resultant potential stays finite which is in contrast to most 1D models, where for infinite acceleration times the ion energies diverge[84]. Although the description of the potential appears to be based on ad hoc assumptions, the model is in excellent agreement (within a factor of 1.5 or so) with experiments performed in a wide range of parameters covering foil thicknesses from one to hundreds of micrometers, laser pulse energies in the sub-joule to kilojoule level, pulse durations from 50 to 5000 fs and ion species covering a major part of the periodic table ranging from protons to tungsten ions. The electric field at the rear side of the target is set up by fast electrons produced by the laser heating at the front side of the target. It should be noted that in general the targets are much thicker than the skin depth or hole-boring depth so that the laser does not interact with the rear of the target. Let us consider that the laser produces N_e electrons with an average energy E_e in a bunch of length $L = c\tau_L$, where τ_L is the laser pulse duration and the electrons are assumed to propagate with the speed of light c. On their way through the target, the electrons spread over a circular region with radius R_s. When exiting into vacuum a positive surface charge Qe is induced at the rear side of the target which yields a returning force $\propto Qe/(\pi R_s^2)$. Electrons run up the potential and eventually reverse their path at a distance z_u above the surface of the foil and re-enter the foil. In an equilibrium situation $2N_e z_u/L$ electrons are permanently outside the foil. To achieve global charge neutrality we identify this number with the number of positive surface charges Q. The potential of the corresponding charge density is

$$\Phi(r,z) = \frac{Qe}{4\pi\varepsilon_0\pi R_s^2}\int_0^{R_s}\int_0^{2\pi}\frac{r'\mathrm{d}r'\mathrm{d}\phi'}{\sqrt{r^2+z^2+r'^2-2rr'\cos\phi'}}. \quad (1)$$

In the following we will concentrate on the center of the acceleration region that is responsible for the most energetic ions, i.e., $r = 0$. In that case the integration of Equation (1) reads

$$-e(\Phi(0,z) - \Phi(0,0)) \equiv -e\Phi(\xi) = E_\infty \left(1 + \xi - \sqrt{1+\xi^2}\right) \equiv E_\infty s(\xi) \quad (2)$$

with

$$E_\infty = \frac{Qe^2}{2\pi\varepsilon_0 R_s} \quad (3)$$

and $\xi = z/R_s$. For short distances $\xi \ll 1$ one has $-e\Phi \cong E_\infty \xi$, which yields for the turning point $z_u = E_e R_s / E_\infty$. The total number of electrons is related to the laser energy E_L by $N_e E_e = \eta E_L$ where η is the efficiency by which the laser energy is converted into electron energy. The electrons are provided for the duration of the laser pulse τ_L. With $Q = 2N_e z_u/(c\tau_L) \propto P_L$ (the power of the laser pulse) we obtain the potential barrier

$$E_\infty = 2m_e c^2 \sqrt{\frac{\eta P_L}{P_{Re}}}. \quad (4)$$

We note that Equation (4) is independent of E_e because $E_\infty \propto Q \propto N_e z_u = (\eta E_L/E_e) \cdot (E_e R_s/E_\infty) = (\eta E_L R_s/E_\infty)$. The essential point is that laser energy is mainly converted into a large number of energetic electrons (fast enough to traverse the target) which in turn build up a dense electron sheath exhibiting extraordinary strong electric fields. It is thus not decisive what average energies E_e are gained by the laser. This is in contrast to the model proposed by Bulanov *et al.*[85] where ions are mainly accelerated by the longitudinal laser electric fields in a bored channel which acts as a waveguide with conducting walls. The potential of Equation (2) can be used to calculate the energy $E_i(\xi)$ an ion with charge q_i gains between $\xi = 0$ (the surface) and ξ:

$$E_i(\xi) = -q_i e\Phi(\xi). \quad (5)$$

The equation of motion yields

$$\tau_L = R_s \int_0^{\xi_m} \frac{\mathrm{d}\xi}{v_i(\xi)} = R_s \int_0^{s_m} \frac{\mathrm{d}\xi/\mathrm{d}s}{v_i(s)} \mathrm{d}s. \quad (6)$$

Now, nonrelativistically one has

$$v_i(s) = v_{i,\infty}\sqrt{s} \quad (7)$$

with $v_{i,\infty} = \sqrt{2E_{i,\infty}/m_i} = c\sqrt{2\varepsilon_{i,\infty}}$. Since

$$\frac{\mathrm{d}\xi}{\mathrm{d}s} = \frac{1+(1-s)^2}{2(1-s)^2}, \quad (8)$$

one obtains

$$\tau_L = \tau_0 \int_0^{s_m} \frac{1+(1-s)^2}{2(1-s)^2\sqrt{s}} \mathrm{d}s = \tau_0 \left[X + \int_0^X \frac{\mathrm{d}x}{(1-x^2)^2}\right] \equiv \tau_0 F_{NR}(X) \quad (9)$$

with $\tau_0 = R_s/v_{i,\infty}$ and $X = \sqrt{s_m} = (E_{i,m}/E_{i,\infty})^{1/2}$. Finally, the integration yields

$$F_{NR}(X) = X + \frac{X}{2(1-X^2)} + \frac{1}{4}\ln\left(\frac{1+X}{1-X}\right) \quad (10)$$

with $X = (\varepsilon_{i,m}/\varepsilon_{i,\infty})^{1/2}$, where $\varepsilon_{i,m} = E_{i,m}/(m_i c^2)$ is the normalized maximum ion energy and $\varepsilon_{i,\infty}$ defines the normalized energy an ion could gain from the potential of the sheath if it were maintained stationary, and is given by $\varepsilon_{i,\infty}(\tau_L) = q_i 2m_e c^2 \sqrt{\eta E_L/(\tau_L P_{Re})}/(m_i c^2) = 1.1 \times 10^{-3}\ (q_i/A_i)\sqrt{\eta E_L/(\tau_L P_{Re})}$. Here, τ_L and E_L are the laser pulse duration and energy respectively, q_i is the ion charge state, A_i is the nucleon number of the target, $P_{Re} = m_e c^3/r_e = 8.71$ GW is the relativistic power unit (r_e = classical electron radius, m_e = electron mass) and η is the absorption efficiency into hot electrons. Following Refs. [86, 87], this efficiency is evaluated as $\eta = 1.2 \times 10^{-15} I_L^{3/4}$, where I_L is in units of W cm^{-2}, up to a maximum $\eta = 0.5$. This scaling has been validated for a laser wavelength of $\lambda_L \sim 1$ µm and pulse durations of several hundreds of femtoseconds. We mention that a similar model has been developed by Bulanov *et al.*[15] who considered a conducting prolate ellipsoid which had been charged up by Q positive charges. The corresponding potential is given by Landau and Lifshitz[88]. However, there exists a major difference from our model: since it is assumed by the ellipsoid model that the surface is conducting, all transverse forces at $z = 0$ have to vanish, which can only be fulfilled by a specific distribution of the Q charges at the surface. However, that can be in contradiction to the laser-driven charge distribution of hot electrons which might be very different from any 'conducting' equilibrium.

One major result of the model presented is that for a given laser energy E_L, the shortest laser pulses and thus highest intensities are not necessarily optimal for TNSA. An important point is that the normalized maximum energy $\varepsilon_{i,\infty}$ an ion can gain depends on the pulse duration τ_L which has a strong consequence on the maximal ion energy $E_{i,m}$. This can be seen in Figure 1(a) where experimental proton energies $E_{i,m}$ (Ref. [57]) are plotted for a constant laser energy $E_L = 0.7$ J as a function of the laser pulse duration τ_L, showing explicitly that there exists an optimal duration τ_L^{opt}. This behavior has been verified on other laser systems as well[89] and can be understood by the following argument. The highest intensity (i.e., shortest pulse) produces the largest acceleration field, but only for a short time. On the other hand, a somewhat smaller field that is sustained over a longer duration of the laser pulse can result in higher ion

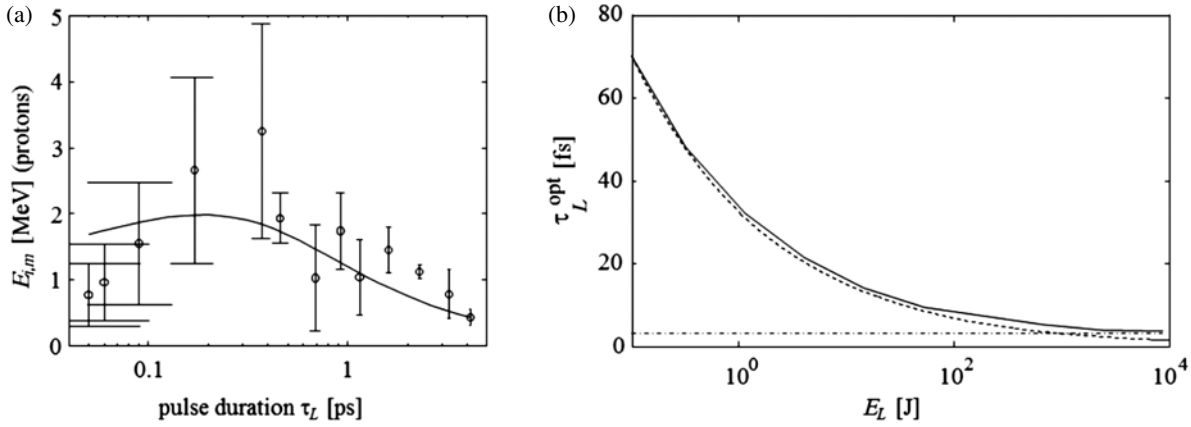

Figure 1. (a) Experimental data from Schreiber *et al.*[57] and the prediction of the nonrelativistic TNSA model. (b) Optimal pulse duration for the specific example of $R_s = 1$ μm, $\eta = 1$, $A_i/q_i = 2$ for the nonrelativistic consideration (Equation (12), dashed) and the relativistic consideration (Equation (29), solid). The ultra-relativistic limit is given by the dash-dotted line. For larger R_s the curves are globally shifted to respective larger optimal pulse durations.

energies. The acceleration is therefore optimized for some intermediate τ_L^{opt}. The solid curve in Figure 1(a) has been obtained from Equation (9) (for details, see Ref. [57]) and is in agreement with the experimental data, thus being able to describe an optimizing procedure. From Equation (9), for fixed laser energy and source radius, one can find the optimum using the condition $\mathrm{d}E_{i,m}/\mathrm{d}\tau_L|_{\tau_L^{\text{opt}}} = 0$. For the nonrelativistic solution, Equation (10), this leads to

$$\left(\frac{\tau_L}{\tau_0}\right)^{\text{opt}} = \frac{X_{\text{opt}}}{3}\left(1 + \frac{1}{(1 - X_{\text{opt}}^2)^2}\right), \tag{11}$$

where X_{opt} is evaluated at $\tau_L = \tau_L^{\text{opt}}$. Insertion of Equations (11) in (10) yields the solution $X_{\text{opt}} \cong 0.81$ with the corresponding value for $(\tau_L/\tau_0)^{\text{opt}} \cong 2.55$. On inserting the nonrelativistic characteristic time τ_0, one obtains for the optimum pulse duration

$$\tau_L^{\text{opt}}(E_L) = 195\left(\frac{R_s}{c}\right)^{4/3}\left(\frac{A_i}{q_i}\right)^{2/3}\left(\frac{P_{Re}}{\eta E_L}\right)^{1/3}. \tag{12}$$

Figure 1(b) shows the optimum pulse duration as a function of the laser energy for $A_i/q_i = 2$, $R_s = 1$ μm and $\eta = 1$. The dashed line is the nonrelativistic solution of Equation (12). The maximum ion energy then becomes

$$(\varepsilon_{i,m}^{\text{opt}})_{\text{TNSA}} = 1.3\frac{q_i}{A_i}\sqrt{\frac{\eta E_L}{\tau_L^{\text{opt}} P_{Ri}}}, \tag{13}$$

where $P_{Ri} = (m_p/m_e)P_{Re} = (1836)^2 P_{Re} = 29.3$ PW is the relativistic power unit for a proton. From Equation (9) it follows that for a given laser system τ_0 should be minimized in order to obtain the largest maximum ion energy $E_{i,m}$. This is realized for the smallest possible source size $R_s = r_L$, where r_L is the radius of the beam spot. Therefore, it is convenient to use targets with thickness d much smaller than the radius of the focal spot, which is usually of the order of some micrometers.

2.2. Relativistic TNSA

The relativistic equation of motion is

$$\frac{\mathrm{d}p_i}{\mathrm{d}t} = q_i e E = -q_i e\frac{\mathrm{d}\Phi}{\mathrm{d}z} \tag{14}$$

with

$$-q_i e\Phi(\xi) = E_{i,\infty}\left(1 + \xi - \sqrt{1+\xi^2}\right) \equiv E_{i,\infty}s(\xi), \tag{15}$$

where $\xi = z/R_s$ and $E_{i,\infty} = q_i 2m_e c^2\sqrt{\eta P_L/P_{Re}}$, as before. The resulting two coupled first-order differential equations

$$\gamma_i^3\frac{\mathrm{d}\beta_i}{\mathrm{d}t^*} = \varepsilon_{i,\infty}\left(1 - \frac{\xi}{\sqrt{1+\xi^2}}\right) \tag{16}$$

and

$$\frac{\mathrm{d}\xi}{\mathrm{d}t^*} = \beta_i \tag{17}$$

have to be solved simultaneously with $t^* = t/t_{0,R} = ct/R_s$ and $\varepsilon_{i,\infty} = E_{i,\infty}/(m_i c^2)$. The initial condition is $t^* = 0$, $\xi = 0$ and $\beta_i = 0$. The ion energy is given by $\varepsilon_i = \gamma_i - 1$ with $\varepsilon_i = E_i/(m_i c^2)$. A first integration of Equation (16) yields

$$\int_0^{\beta_i}\gamma_i^3\beta_i\mathrm{d}\beta_i = \varepsilon_{i,\infty}\int_0^{\xi}\frac{\mathrm{d}s}{\mathrm{d}\xi'}\mathrm{d}\xi' \tag{18}$$

or

$$\gamma_i - 1 = \varepsilon_i = \varepsilon_{i,\infty}s(\xi). \tag{19}$$

Now, instead of Equation (7) one has

$$v_i(s) = c\sqrt{1-(1+\varepsilon_{i,\infty}s)^{-2}} \tag{20}$$

and thus

$$\frac{\tau_L}{\tau_{0,R}} = \int_0^{s_m} \frac{1+(1-s)^2}{2(1-s)^2\sqrt{1-(1+\varepsilon_{i,\infty}s)^{-2}}}\mathrm{d}s \tag{21}$$

with $\tau_{0,R} = R_s/c$ and $s_m = E_{i,m}/E_{i,\infty} = \varepsilon_{i,m}/\varepsilon_{i,\infty} = X^2$. It is immediately seen from Equation (21) that deviations from nonrelativistic TNSA occur for $\varepsilon_{i,\infty}s_m = \varepsilon_{i,m} \geqslant 1$ (compare Equation (9)).The essential difference is that nonrelativistically the final ion velocity $v_{i,\infty}$ might become arbitrarily large, but special relativity limits it to the speed of light. We note that Equation (21) can be written as

$$\begin{aligned}\frac{\tau_L}{\tau_0} &= \sqrt{2\varepsilon_{i,\infty}}\int_0^{s_m} \frac{1+(1-s)^2}{2(1-s)^2\sqrt{1-(1+\varepsilon_{i,\infty}s)^{-2}}}\mathrm{d}s \\ &\equiv F_R(X;\varepsilon_{i,\infty}).\end{aligned} \tag{22}$$

As a relativistic first-order correction to Equation (22) one obtains

$$\begin{aligned}\frac{\tau_L}{\tau_0} &= \int_0^X \frac{1+(1-x^2)^2}{(1-x^2)^2}\mathrm{d}x \\ &\quad - \frac{\varepsilon_{i,\infty}}{4}\int_0^X \frac{x^2(1+(1-x^2)^2)}{(1-x^2)^2}\mathrm{d}x \\ &= X + \frac{X}{2(1-X^2)} + \frac{1}{4}\ln\frac{1+X}{1-X} \\ &\quad - \frac{\varepsilon_{i,\infty}}{4}\left(\frac{X^3}{3} + \frac{X}{2(1-X^2)} - \frac{1}{4}\ln\frac{1+X}{1-X}\right).\end{aligned} \tag{23}$$

Unfortunately the simple scaling of Equation (9) is lost since now in F_R the additional parameter $\varepsilon_{i,\infty}$ accounts for relativistic effects. Using the value of $X_{\mathrm{opt}} \cong 0.8$ of the nonrelativistic TNSA expression as a first-order solution we obtain a condition for the optimized pulse duration in the case of relativistic TNSA:

$$\left(\frac{\tau_L}{\tau_0}\right)^{\mathrm{opt}} = 2.5 - 0.18\varepsilon_{i,\infty}^{\mathrm{opt}} \tag{24}$$

or

$$\frac{c\sqrt{a}}{R_s}(\tau_L^{\mathrm{opt}})^{3/4} = 2.5 - \frac{0.18a}{(\tau_L^{\mathrm{opt}})^{1/2}} \tag{25}$$

with $a = 1.1\times10^{-3}(q_i/A_i)\sqrt{\eta E_L/P_{Re}}$. An analytic solution of Equation (25) reads

$$a = \frac{2.5}{\alpha_2} + \left(\frac{\alpha_1}{\alpha_2}\right)^2\left[1-\sqrt{1+\frac{5\alpha_2}{\alpha_1^2}}\right] \tag{26}$$

with $\alpha_1 = c(\tau_L^{\mathrm{opt}})^{3/4}/R_s$ and $\alpha_2 = 0.18/(\tau_L^{\mathrm{opt}})^{1/2}$. The nonrelativistic TNSA-limit Equation (11) is obtained for $\alpha_2 \to 0$:

$$a \cong \frac{25}{8\alpha_1^2} - \frac{125}{16\alpha_1^4}\alpha_2 = \frac{3.1R_s^2}{c^2(\tau_L^{\mathrm{opt}})^{3/2}}\left(1-0.45\left(\frac{R_s}{c\tau_L^{\mathrm{opt}}}\right)^2\right). \tag{27}$$

Again, the nonrelativistic optimal ion energy $(\varepsilon_{i,m}^{\mathrm{opt}})_{\mathrm{TNSA}}$ is obtained by Equation (13). The term within the bracket is the relativistic correction. A few things are worthy of note. (1) The correction due to relativistic ion motion becomes larger with decreasing optimal pulse duration, that is for larger laser energy E_L. This can be expected. However, (2) the correction decreases the value of a; in other words, the optimum pulse duration τ_L^{opt} is reduced even when the laser energy E_L remains constant. This in turn means that the optimum ion energy becomes larger if relativistic corrections are taken into account. (3) The correction increases with increasing R_s. Nonrelativistically τ_L^{opt} increases with $R_s^{4/3}$ (see Equation (12)), but relativistically this increase is less strong.

Writing Equation (21) as

$$\frac{\tau_L}{\tau_{0,R}} = \int_0^{s_m} H(s;\varepsilon_{i,\infty})\mathrm{d}s \tag{28}$$

and optimizing Equation (28) by the condition $\mathrm{d}\varepsilon_{i,m}/\mathrm{d}\tau_L|_{\tau_L^{\mathrm{opt}}} = 0$ yields

$$\frac{1}{\tau_{0,R}} = \frac{\mathrm{d}s_m}{\mathrm{d}\tau_L}H(s_m;\varepsilon_{i,\infty}) + \int_0^{s_m}\frac{\partial}{\partial\tau_L}H(s,\varepsilon_{i,\infty})\mathrm{d}s. \tag{29}$$

It follows that

$$\frac{\mathrm{d}s_m}{\mathrm{d}\tau_L} = \frac{\mathrm{d}\varepsilon_{i,m}}{\mathrm{d}\tau_L}\frac{1}{\varepsilon_{i,\infty}} - \frac{\varepsilon_{i,m}}{\varepsilon_{i,\infty}^2}\frac{\mathrm{d}\varepsilon_{i,\infty}}{\mathrm{d}\tau_L} = \frac{s_m}{2\tau_L} \tag{30}$$

and

$$\begin{aligned}\frac{\partial H}{\partial\tau_L} &= \frac{1}{4\tau_L}\frac{1+(1-s)^2}{(1-s)^2} \\ &\quad\times\frac{\varepsilon_{i,\infty}s}{(1+\varepsilon_{i,\infty}s)^3(1-(1+\varepsilon_{i,\infty}s)^{-2})^{3/2}}.\end{aligned} \tag{31}$$

One therefore has the condition

$$\begin{aligned}4\frac{\tau_L^{\mathrm{opt}}}{\tau_{0,R}} &= \frac{s_m^{\mathrm{opt}}(1+(1-s_m^{\mathrm{opt}})^2)}{(1-s_m^{\mathrm{opt}})^2\sqrt{1-(1+\varepsilon_{i,\infty}^{\mathrm{opt}}s_m^{\mathrm{opt}})^{-2}}} \\ &\quad + \int_0^{s_m^{\mathrm{opt}}}\frac{1+(1-s)^2}{(1-s)^2} \\ &\quad\times\frac{\varepsilon_{i,\infty}^{\mathrm{opt}}s}{(1+\varepsilon_{i,\infty}^{\mathrm{opt}}s)^3(1-(1+\varepsilon_{i,\infty}^{\mathrm{opt}}s)^{-2})^{3/2}}\mathrm{d}s \\ &= 4\int_0^{s_m^{\mathrm{opt}}}\frac{1+(1-s)^2}{2(1-s)^2(1-(1+\varepsilon_{i,\infty}^{\mathrm{opt}}s)^{-2})^{1/2}}\mathrm{d}s,\end{aligned} \tag{32}$$

where $s_m^{\rm opt} = \varepsilon_{i,m}^{\rm opt}/\varepsilon_{i,\infty}^{\rm opt}$ and $\varepsilon_{i,\infty}^{\rm opt} = 1.1 \times 10^{-3}(q_i/A_i)\sqrt{\eta E_L/(\tau_L^{\rm opt} P_{Re})}$. A numerical solution yields $s_m^{\rm opt}$ with $\varepsilon_{i,\infty}^{\rm opt}$ as a parameter. By inserting these solutions into Equation (29) one obtains the required $\tau_L^{\rm opt}/\tau_{0,R}$ (solid line in Figure 1(b)) and $\varepsilon_{i,m}^{\rm opt}$.

In the highly relativistic regime, the ion velocity approaches the speed of light for approximately all the acceleration time, which according to Equation (6) leads to

$$\frac{\tau_L}{\tau_{0,R}} = \xi_m \tag{33}$$

or

$$\varepsilon_{i,m} = 1.1 \times 10^{-3}(q_i/A_i)\sqrt{\frac{\eta E_L}{m_e c^2}\frac{R_s}{r_e}}\,G(\xi_m) \tag{34}$$

with

$$G(\xi_m) = \left(1 + \xi_m - \sqrt{1+\xi_m^2}\right)\Big/\sqrt{\xi_m}. \tag{35}$$

The function $G(\xi_m)$ has a rather broad maximum at $\xi_m = \tau_L^{\rm opt} c/R_s = 1$. Whereas in the nonrelativistic regime the optimum pulse duration decreases with increasing laser energy E_L, see Equation (12), it becomes a constant, $\tau_L^{\rm opt} = R_s/c$, for relativistic ion energies (dash-dotted line in Figure 1(b)). On inserting the value for G one obtains from Equation (34) the optimal ion energy

$$(\varepsilon_{i,m}^{\rm opt})_{\rm TNSA} = 0.64 \times 10^{-3}(q_i/A_i)\sqrt{\frac{\eta E_L}{m_e c^2}\frac{R_s}{r_e}}. \tag{36}$$

We conclude this section with two remarks. (i) The ion energy $E_{i,m}$ is a unique function of E_L and τ_L, i.e., for constant laser energy a function of τ_L only. Thus, $E_{i,m}$ might show a maximum with respect to τ_L or not. However, if there exists a maximum it is unique, i.e., there is a single-valued $E_{i,m}^{\rm opt} = E_{i,m}(\tau_L^{\rm opt})$ only. (ii) We propose a simple equation for the whole range,

$$\varepsilon_{i,m} = 1.3 \cdot \varepsilon_{i,\infty}\left(1 + \frac{\tau_L}{\tau^*} - \sqrt{1 + \left(\frac{\tau_L}{\tau^*}\right)^2}\right), \tag{37}$$

with

$$\tau^* = \frac{R_s/c}{\sqrt{1 - \frac{1}{(1+\varepsilon_{i,\infty})^2}}}. \tag{38}$$

It might be that a better approximation is obtained if in the last equation $\varepsilon_{i,\infty}$ is replaced by $\varepsilon_{i,m}$. Bulanov *et al.*[85] have performed detailed PIC studies of the generation of high energy ions in overcritical targets. For strong focusing conditions ($R_s \cong 0.75$ μm), they obtained for $P_L = 1$ PW and a pulse duration of $\tau_L = 30$ fs (i.e., a laser energy of $E_L = 30$ J) a proton energy of 1.3 GeV. With $\varepsilon_{i,\infty} = 0.37$ and $\tau^* = 3.6$ fs we obtain from Equation (37) $E_{i,m} = 430$ MeV.

3. Radiation pressure acceleration

At the intensities available with present high-intensity lasers, it seems natural to consider RPA as a means of accelerating objects to high energy. RPA offers the most promising approach for the acceleration of plasma bunches with near-solid, or at least overcritical, density to relativistic velocities. The principle of RPA is the same as was proposed to use continuous wave lasers to drive interstellar vehicles to relativistic velocities[31, 50]. According to Simmons *et al.*[31], a body with rest mass comparable to the applied laser energy can be accelerated close to the speed of light. For a 5 nm thin carbon foil and a focal spot diameter of 2 μm, this would require only 5 J of energy. Unfortunately, the picture is not quite as simple due to the immense intensity of the applied laser. In Section 2, we have highlighted the importance of a high rate of absorption of laser energy into hot electrons for TNSA. For hole-boring or RPA to work efficiently, this heating must be suppressed, which may be achieved by the use of high-contrast systems with circular polarization[34]. In this way the ponderomotive force that acts on the plasma electrons is only composed of a secular term which can effectively expel the electrons from the focal region and push them into the target. The space charge separation in the focal region is then maintained over the duration of the laser pulse, or even longer when the reflection front starts to move. During this time, electrons stay cold, i.e., they do not gain a large longitudinal momentum spread, so they stay bound to this initial depletion zone.

The acceleration of an object with mass $M = m_i n_i {\rm d}\pi r_L^2$ by the radiation pressure, where n_i is the ion particle density, is described by Refs. [31, 34, 35]

$$\frac{{\rm d}(\gamma\beta)}{{\rm d}t} = \frac{1}{t_0}\frac{1-\beta}{1+\beta}, \tag{39}$$

where $t_0 = Mc^2/(2RP_L)$ and R denotes the reflectivity with which the laser is reflected. For a constant laser power P_L, a solution of Equation (39) in terms of the actual time t is not of much interest because of the retardation effect. More relevant is a solution in terms of the retarded time $t_{\rm ret} = t - \int_0^t \beta(t'){\rm d}t'$ (Refs. [31, 34]). Thus, Equation (39) becomes

$$\frac{{\rm d}\beta}{{\rm d}t_{\rm ret}} = \frac{1}{t_0}\frac{1-\beta}{\gamma}, \tag{40}$$

with the solution for the normalized ion energy

$$\varepsilon_{i,m}^{\rm RPA} = \gamma - 1 = \frac{1}{2}\left(1 + \zeta + \frac{1}{1+\zeta}\right) - 1, \tag{41}$$

where $\zeta = t_{\rm ret}/t_0 = 2RE_L/(Mc^2)$, since the light pulse is terminated at the retarded time $t_{\rm ret} = \tau_L$. We note that the interaction between the light and the plasma sheet may continue even when the laser has finished radiating: for relativistic velocities of the sheet the light pulse accompanies the bunch for interaction times $t = t_{\rm int}$ much longer than the pulse duration

$$t_{\rm int} = \tau_L \left(1 + \frac{\zeta}{2} + \frac{\zeta^2}{6}\right). \tag{42}$$

The essential point for the RPA mechanism is the assumption that the whole target of mass M is accelerated cooperatively as a charge-neutral plasma bunch. The physical mechanism behind this process is the following. Due to their small mass the electrons are accelerated by light pressure and then due to Coulomb forces drag the ions behind them (hence the name light-sail[43, 90]). Thus, one has to avoid the light pressure on the electrons exceeding the restoring forces due to the charge separation.

On inspecting Equation (41) it is readily seen that the ion energy $E_{i,m}^{\rm RPA}$ increases with ζ and thus with decreasing target mass M, or with thinner target foils. However, a lower limit will be reached if the number of ions becomes so small that they cannot any longer retain the electrons by their Coulomb forces. One estimates the energy E_∞ to separate an electron from a sheet of ion charge density $q_i n_i = n_e$ to be $E_\infty = n_e {\rm d} r_L e^2/(4\varepsilon_0)$ (Ref. [57]). This estimate can also be derived from the 'capacitor' model for charge separation[37, 38, 91] assuming an effective cut-off of the induced electric field for distances larger than the lateral extension of the sheet. This assumption is equivalent to the demand to maintain the balance between charge separation and radiation pressure at least over a laser period[81, 92]. Evidently, the charge separating energy increases with the areal density $n_i d$ while the radiation pressure decreases like $(n_i d)^{-1}$, advocating once more the use of ultra-thin targets. The ion energy can be derived from Equation (41) in the nonrelativistic case $E_{i,m} \propto \zeta^2 \propto 1/M^2 \propto 1/d^2$. For a completely ionized carbon target with a thickness of 1 μg cm^{-2} one obtains $E_\infty \cong 10$ MeV. On the other hand, this estimate shows that there exists a lower limit on the electron mass M_e that can be accelerated by radiation pressure and which remains bound to the ions. The latter demand is essential for ion acceleration since it is the electrons that pull the ions behind them. If M_e becomes too small, the resulting fast electrons with energies $E_e = m_e c^2 \gamma \cong m_e c^2 \tau_L/(2t_0) = (m_e/M_e)E_L = E_L/N_e$ (note that at large electron energies the efficiency approaches 100%, i.e., all the laser energy is converted into the kinetic energy of N_e electrons) can surmount the potential barrier built up by the charge separation field (note that $M_e = m_e n_e {\rm d} r_L^2$). Thus, the minimum ion mass that prohibits charge separation and that can be accelerated as a charge-neutral plasma bunch

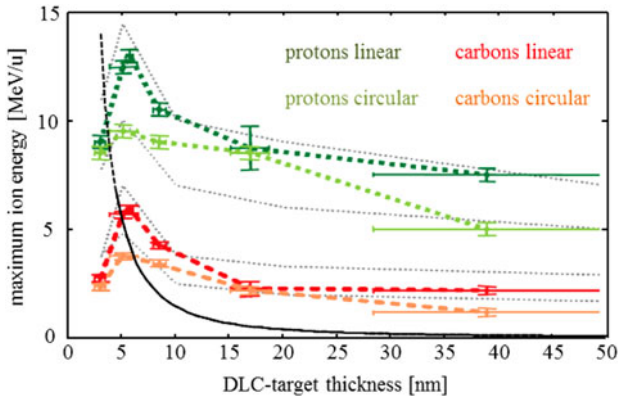

Figure 2. Maximum proton and carbon ion energies for varying thicknesses of nm-thin DLC foils reported in Henig *et al.*[51]. The solid curve represents the prediction for RPA, Equation (41), using the parameters $A_i/q_i = 2$, $E_L = 0.7$ J, $r_L = 1.8$ μm, $R = 1$, $\rho_{\rm DLC} = 2.7$ g cm^{-3}. The optimum mass/thickness is indicated by the transition of the solid to a dashed curve.

becomes

$$M_{\rm min} = \frac{A_i}{q_i}\sqrt{\frac{4\varepsilon_0 E_L r_L}{e^2}}\, m_u \tag{43}$$

with the atomic mass unit m_u and A_i the mass number of the target. For a carbon target with $A_i/q_i = 2$, $E_L = 1$ J and $r_L = 3$ μm one obtains $M_{\rm min} = 2.2 \times 10^{-16}$ kg, corresponding to an optimum thickness of 4 nm. This is in strong contrast to a TNSA model of Andreev *et al.*[93] who predicted an optimum thickness of about 100 nm. In Refs. [51, 94] the maximum ion energy has been investigated as a function of the target mass M. As expected, the ion energy increases with $1/M$, but for masses close to $M_{\rm min}$ the energy starts to drop rather strongly with further decreasing target masses, thus confirming the estimate of Equation (43) quantitatively. Figure 2 reproduces the experimental results of Ref. [51] for the carbon energies obtained from nm-thin diamond-like carbon (DLC) foils. The solid curve has been obtained from Equation (41). Although the curve drops off faster towards thicker targets (due to the increasing domination of expansion), evidently there exists an optimal foil thickness, i.e., target mass. The estimate of Equation (43) is indicated where the solid line breaks into the dashed line. An estimate of the optimal and thus minimum foil thickness by Chen *et al.*[95] is in essence the same as that of Equation (43).

In a very recent theory of laser ion acceleration from thin foils[96] the dimensionless parameter

$$\xi = \frac{n_e {\rm d}}{n_c \lambda a_0} \tag{44}$$

has been introduced, which for small laser strength a_0 and thus $\xi \geqslant 1$ prohibits charge separation, i.e., allows collective ion acceleration induced by electrons riding ahead of the ions. Here, n_c is the critical electron density. It is easy to show that Equation (44) can also be written as $\xi =$

$M/M_{\min}$ with $M_{\min}$ of Equation (43). Thus, the condition $\xi \geqslant 1$ for an appropriate ion acceleration is equivalent to demanding $M \geqslant M_{\min}$. Identifying $M_{\min}$ with the optimal target mass M_{opt} for RPA and inserting Equations (43) into (41) one obtains $(\varepsilon_{i,m}^{\text{opt}})_{\text{RPA}}$, which can be compared with the equivalent expression for the case of optimal TNSA. In Figure 3 $\varepsilon_{i,m}^{\text{opt}}$ has been plotted for either TNSA or RPA versus the laser energy E_L. The curves hold for $R_s = r_L = 1$ μm (solid lines) and $R_s = r_L = 10$ μm (dashed lines), $A_i/q_i = 2$ and $\eta = R = 1$. For a typical high-intensity laser with a wavelength of $\lambda_L = 1$ μm, a beam spot radius of 1 μm is close to the diffraction-limited minimum sized beam spot. The corresponding data in Figure 3 thus represent optimum ion energies also within this context. The extension of available laser energies up to 10 kJ might be optimistic but we note that in a recent paper by Tajima *et al.*[5] on electron acceleration up to PeV even GJ laser energies have been discussed. A laser with $E_L = 1$ GJ could accelerate by radiation pressure a carbon foil of optimal thickness of 300 μm with C ions in it up to energies of 60 TeV/ion ($\gamma = 5 \times 10^3$, which is close to the heavy-ion energies of CERN's Large Hadron Collider[97]). However, we also note that for a pulse duration of 1 ps[5], the interaction distance according to Equation (42) would become 5 km. The reflected radiation has a vanishingly small frequency and at the end of the acceleration process nearly all the laser pulse energy is converted into kinetic energy of the ions, $E_L \cong (\gamma - 1)M_{\text{opt}}c^2$, see also Equation (45). It would not be easy to stop such an ion bunch. Its energy content is large enough to heat up and finally melt 15 tons of lead. For comparison, the 7.7 TeV protons stored in the LHC have an energy content of 0.6 GJ[98]. An elegant solution of such a 'beam-dump' problem has recently been proposed by Wu *et al.*[99], relying on the deceleration of energetic and dense particle bunches by collective electronic interactions in an underdense plasma, promising a compact and non-radioactive dump. However, two remarks might be made. (i) The main contribution to the energy loss of ultra-relativistic heavy ions is electron–positron pair creation and not electronic stopping ('Bethe–Bloch')[97]. According to the description of Ref. [97] we obtain for the case discussed – 60 TeV carbon ions in lead – an electronic energy loss of 0.07 TeV m^{-1} and one by pair production of 0.3 TeV m^{-1}. Energy losses due to bremsstrahlung can be neglected since the small impact parameters necessary to generate hard photon quanta lead unavoidably to a fragmentation of the projectile[97]. We thus estimate for the example mentioned above a stopping length of about 570 m. In contrast, a beam-dump length of several meters only is sufficient to break up the projectile by nuclear inelastic interactions, yielding a cascade of secondary particles with individual energies much less than the primary one[100]. It is mainly the electromagnetic component of the cascade that finally converts the energy into heat. (ii) The essential point

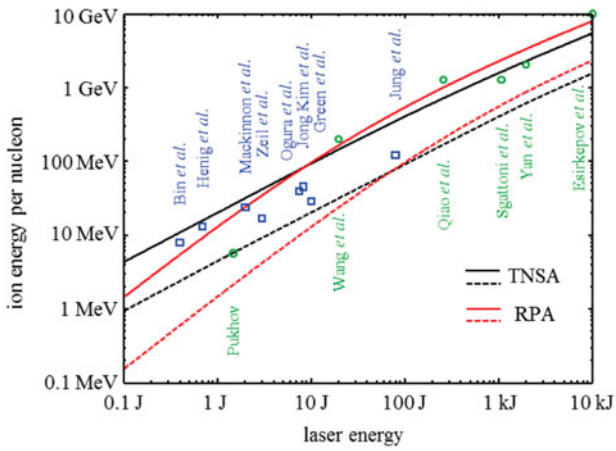

Figure 3. Optimum ion energies predicted by the models for TNSA, Equations (29)–(32) (black), and RPA, Equations (41)–(43) (red). The parameters are $A_i/q_i = 2$, $R = \eta = 1$, $r_L = R_s = 1$ μm (solid) and $r_L = R_s = 10$ μm (dashed). Some selected experimental results are represented by blue squares (Bin *et al.*[112], Henig *et al.*[51], Mackinnon *et al.*[108], Zeil *et al.*[113], Ogura *et al.*[68], Jong Kim *et al.*[114], Green *et al.*[115], Jung *et al.*[116]) and theoretical results obtained from PIC simulations are marked by green circles (Pukhov[71], Wang *et al.*[117], Qiao *et al.*[40], Sgattoni *et al.*[118], Yan *et al.*[75], Esirkepov *et al.*[35]). For details, see text.

is not to stop the bunch within a moderate distance and thus heat the absorber but to dissipate its enormous energy concentration without any further problem. The situation for a laser-generated ion bunch is quite different from that of the LHC where the particles are more or less homogeneously distributed around the 27 km long circumference of the storage ring: C ions within a bunch length of 300 μm compared with 5×10^{14} protons stored within 27 km. The corresponding pulse length of 90 μs is long enough to allow kicker magnets to sweep the beam across the absorber.

It is readily seen that except for a minor factor over the whole range of laser energies both optimized theories yield the same maximum ion energies. It is therefore more a question of practicability what kind of optimization one chooses, τ_L^{opt} or M_{opt}. There might exist technical limits: it is certainly very difficult to obtain pulse durations shorter than say 1 fs. According to Equation (29) this would correspond to an upper limit of $E_L = 3 \times 10^4$ J, which in essence does not pose a strong limit. On the other hand, in the case of RPA a lower limit of M_{opt} is reached for a monolayer of atoms. Assuming a carbon foil as the target (the most popular choice) one obtains a lower limit of $M_{\text{opt}} = 1.4 \times 10^{-18}$ kg, or from Equation (41) a lower limit of $E_L = 1.3 \times 10^{-4}$ J, which also does not have a practical influence. We emphasize that the optimizing procedure developed in this paper only works since the TNSA theory of Schreiber *et al.*[57] does not depend on the target thickness (at least to first order) and the RPA theory of Refs. [35, 101, 102] does not depend on the pulse duration.

In addition, experimental results are plotted in Figure 3 demonstrating that in most cases experiments are rather far

away from being optimal. Multi-J laser systems especially suffer from having too long a pulse duration. We also note that normalized ion energies $\varepsilon_{i,m} \geqslant 1$ or $E_{i,m} \geqslant 1$ GeV/u, i.e., relativistic energies, are obtained for laser energies $E_L \geqslant 100$ J only and so far have only been obtained in PIC simulations. Finally, we note that the efficiency of RPA can be written as

$$\eta_{\mathrm{RPA}} \equiv \frac{E_{i,m}}{E_L} = \frac{R\zeta}{1+\zeta}, \tag{45}$$

i.e., in the relativistic regime with $\gamma \gg 1$ or with Equation (41) $\zeta \gg 1$ one obtains that for $R = 1$, 100% of the laser energy is converted into ion energy.

Of course, if the transverse light intensity changes, different parts of the sail will be accelerated differently changing an initially plane sail to a convex one. The equation of motion of Equation (39) changes to

$$\frac{\mathrm{d}(\gamma\vec{\beta})}{\mathrm{d}t} = \frac{2RP_L}{Mc^2}\frac{1-\beta}{1+\beta}\vec{n}, \tag{46}$$

where both $P_L = P_L(y,z;t)$ and the unit vector $\vec{n} = \vec{n}(y,z;t)$ of the sail's surface normal depend on the transverse coordinates (y,z) and time t. Thus, a solution of Equation (46) has to account for a transverse expansion of the sail. An approximate solution of this self-consistent problem to obtain both the final velocity β and the shape of the sail, allowing for bowing while simultaneously submitting it to the condition of constant mass, has been given in Ref. [103]. The essential point is that instabilities like those of the Rayleigh–Taylor type lead to strong deviations from a uniform plasma front, forming cusps at an early stage of acceleration[104], resulting in emission of beamlets[105]. To avoid such instabilities Chen *et al.*[95] have proposed to use thin target foils shaped initially in the transverse direction to match the laser intensity profile. PIC simulations by Wilks *et al.*[106] performed as far back as in 1992 clearly demonstrated such instabilities for light intensities relevant to the light-sail regime. However, we remark that the ion energy differs for every beamlet. At a later stage the 'plasma foil' breaks into high-density clumps with diffuse lower density clouds between them[104], which due to its reduced mass may even accelerate ions to higher energies than the original foil[103]. A similar result has been obtained quite recently, demonstrating by PIC simulations that 'a relatively stable ion clump forms near the laser axis which is efficiently accelerated'[75]. A detailed study of Rayleigh–Taylor instabilities which yield filamentation and their optimization with respect to maximum ion energies has been published recently[85, 107].

4. Discussion

We are very much aware that analytic descriptions of the complex laser-assisted acceleration process of ions are hampered in many aspects. In contrast, PIC simulations describe in much more detail the complex processes described here. However, we also believe that an analytic description of the multi-parameter behavior of the process and its interdependences can give a more general overlook of the strategy to obtain the required outcomes such as, e.g., maximum ion energies. At the same time we remark that also PIC simulations which in essence are based on a mean field theory may rather severely suppress microscopic interactions. We also recognize a significant overshoot of PIC simulations, promising ion beams of great quality not verified by experiment hitherto. We cite a very recent paper: 'as pointed out recently in a number of papers circular polarized laser pulses can accelerate ions very efficiently and produce sharply peaked spectra'[75]. This hope results from PIC simulations only and still awaits experimental verification. In the following we will touch on some problems not considered in the analytic description. First, there is the question of the longitudinal and transverse extension of the laser beam. It has been assumed that the laser power is constant during its pulse duration, but even the use of a super-Gauss representation of the time dependence would merely change the conclusions. This might be rather different for the transverse extent which for a mono-mode laser system is Gaussian. In the case of TNSA this effect yields an electron sheet with transversely changing field strength which accelerates ions to different energies. Such broad spectra are not very favorable for specific applications. A similar problem arises in the case of RPA. The solution Equation (41) assumes that the light pressure is in essence transversely constant. RPA for a transverse Gaussian light beam has been investigated in detail by Bulanov *et al.*[92, 103] with PIC simulations showing in particular the buckling of an initially flat foil. Although the RPA process itself seems to remain stable, a rather broad ion spectrum results in this case also.

We note that such high energies as predicted by the analytical models have not been observed yet even though comparable laser conditions have been applied, for example by Mackinnon *et al.*[108]. Proton energies of up to 25 MeV have been obtained in the TNSA regime with micrometer thick targets. The discrepancy may be attributed to an absorption of laser energy into electrons much below 100%, especially when considering the high temporal contrast employed. The results could also be an indication that the electrons spread transversely over a size larger than $R_s \cong r_L$, even though the target thickness d was smaller than r_L in those experiments.

Hence, the studies presented here are encouraging in view of future applications that rely on high-repetition-rate laser systems. For example, for medical applications such as ion tumor therapy energies exceeding 100 MeV/u are envisioned. This energy range should be attainable even with sub-100 J laser systems, while relativistic energies can be achieved with energies slightly above 100 J. In

order to increase the ion energy even further, i.e., above the multi-GeV level, kJ systems such as envisioned for the Extreme Light Infrastructure will be necessary. It may also become necessary to consider novel methods not discussed here. For example, once the ions move with the speed of light, staged acceleration possibly implementing plasma wake acceleration as used presently to accelerate electrons may provide a more effective means to reach higher energies[109–111]. In any case, even with lower output ion energies as compared with conventional accelerators, laser-accelerated ion bunches are still desirable, due to their bunch densities which may be close to solid density. Even with the low repetition rate of most high-power laser systems, the high number of reactions per unit volume that would be achievable with solid density bunches is perfectly suited for the exploration of the field of nonlinear nuclear physics, such as the production of exotic nuclei by fission–fusion reactions. Another important feature is the possible short ion bunch duration paired with the synchronism to other laser-driven radiation sources to allow for time- and space-resolved studies in pump–probe schemes.

5. Summary

Starting from experimental results, we have shown that current theories of laser–ion acceleration can and should be optimized in order to achieve maximum ion energies. Not all theories include such a possibility, but the TNSA theory of Schreiber *et al.*[57] can be optimized with respect to laser pulse duration and the RPA theory of Bulanov *et al.*[35, 101, 102] with respect to target thickness. It turns out that both the optimized TNSA and RPA theories yield approximately the same maximum ion energies over the range of laser energies 0.1 J $< E_L <$ 10 kJ. It is thus a matter of convenience whether one adjusts the optimal pulse duration or the optimal target thickness. For both theories, the decisive laser parameter is neither the power nor the intensity but solely the laser energy. Relativistic ion energies, i.e., energies beyond 1 GeV/u, can be obtained for systems with $E_L > 100$ J, where in addition a diffraction-limited small spot size has to be achieved.

Acknowledgements

This work was supported by the DFG Cluster of Excellence Munich Centre for Advanced Photonics (MAP) and the Transregio 18 as well as the Euratom/toIFE-project at MPQ. The authors thank Dr. Claudio Bellei for valuable and fruitful discussions.

References

1. H. Daido, M. Nishiuchi, and A. S. Pirozhkov, Rep. Progr. Phys. **75**, 056401 (2012).
2. A. Macchi, M. Borghesi, and M. Passoni, Rev. Modern Phys. **85**, 751 (2013).
3. T. E. Cowan, J. Fuchs, H. Ruhl, A. Kemp, P. Audebert, M. Roth, R. Stephens, I. Barton, A. Blazevic, E. Brambrink, J. Cobble, J. Fernández, J.-C. Gauthier, M. Geissel, M. Hegelich, J. Kaae, S. Karsch, G. P. Le Sage, S. Letzring, M. Manclossi, S. Meyroneinc, A. Newkirk, H. Pépin, and N. Renard-LeGalloudec, Phys. Rev. Lett. **92**, 204801 (2004).
4. M. Kando, H. Kiriyama, J. K. Koga, S. Bulanov (JAERI, Kyoto), A. W. Chao (SLAC), T. Esirkepov, R. Hajima, and T. Tajima, AIP Conf. Proc. **1024**, 197 (2008).
5. T. Tajima, M. Kando, and M. Teshima, Progr. Theoret. Phys. **125**, 617 (2011).
6. B. M. Hegelich, B. J. Albright, J. Cobble, K. Flippo, S. Letzring, M. Paffett, H. Ruhl, J. Schreiber, R. K. Schulze, and J. C. Fernández, Nature **439**, 441 (2006).
7. H. Schwoerer, S. Pfotenhauer, O. Jackel, K. U. Amthor, B. Liesfeld, W. Ziegler, R. Sauerbrey, K. W. Ledingham, and T. Esirkepov, Nature **439**, 445 (2006).
8. S. Ter-Avetisyan, M. Schnurer, P. V. Nickles, M. Kalashnikov, E. Risse, T. Sokollik, W. Sandner, A. Andreev, and V. Tikhonchuk, Phys. Rev. Lett. **96**, 145006 (2006).
9. S. M. Pfotenhauer, O. Jäckel, A. Sachtleben, J. Polz, W. Ziegler, H.-P. Schlenvoigt, K.-U. Amthor, M. C. Kaluza, K. W. D. Ledingham, R. Sauerbrey, P. Gibbon, A. P. L. Robinson, and H. Schwoerer, New J. Phys. **10**, 033034 (2008).
10. A. P. Fews, P. A. Norreys, F. N. Beg, A. R. Bell, A. E. Dangor, C. N. Danson, P. Lee, and S. J. Rose, Phys. Rev. Lett. **73**, 1801 (1994).
11. M. Roth, T. E. Cowan, M. H. Key, S. P. Hatchett, C. Brown, W. Fountain, J. Johnson, D. M. Pennington, R. A. Snavely, S. C. Wilks, K. Yasuike, H. Ruhl, F. Pegoraro, S. V. Bulanov, E. M. Campbell, M. D. Perry, and H. Powell, Phys. Rev. Lett. **86**, 436 (2001).
12. P. K. Patel, A. J. Mackinnon, M. H. Key, T. E. Cowan, M. E. Foord, M. Allen, D. F. Price, H. Ruhl, P. T. Springer, and R. Stephens, Phys. Rev. Lett. **91**, 125004 (2003).
13. S. V. Bulanov and V. S. Khoroshkov, Plasma Phys. Rep. **28**, 453 (2002).
14. E. Fourkal, B. Shahine, M. Ding, J. S. Li, T. Tajima, and C. M. Ma, Med. Phys. **29**, 2788 (2002).
15. S. V. Bulanov, H. Daido, T. Z. Esirkepov, V. S. Khoroshkov, J. Koga, K. Nishihara, F. Pegoraro, T. Tajima, and M. Yamagiwa, AIP Conf. Proc. **740**, 414 (2004).
16. V. Malka, S. Fritzler, E. Lefebvre, E. d'Humières, R. Ferrand, G. Grillon, C. Albaret, S. Meyroneinc, J. Chambaret, A. Antonetti, and D. Hulin, Med. Phys. **31**, 1587 (2004).
17. U. Linz and J. Alonso, Phys. Rev. ST Accel. Beams **10**, 094801 (2007).
18. L. Romagnani, J. Fuchs, M. Borghesi, P. Antici, P. Audebert, F. Ceccherini, T. Cowan, T. Grismayer, S. Kar, A. Macchi, P. Mora, G. Pretzler, A. Schiavi, T. Toncian, and O. Willi, Phys. Rev. Lett. **95**, 195001 (2005).
19. L. Romagnani, S. V. Bulanov, M. Borghesi, P. Audebert, J. C. Gauthier, K. Löwenbrück, A. J. Mackinnon, P. Patel, G. Pretzler, T. Toncian, and O. Willi, Phys. Rev. Lett. **101**, 025004 (2008).
20. T. Sokollik, M. Schnürer, S. Ter-Avetisyan, P. V. Nickles, E. Risse, M. Kalashnikov, W. Sandner, G. Priebe, M. Amin, T. Toncian, O. Willi, and A. A. Andreev, Appl. Phys. Lett. **92**, 091503 (2008).
21. P. A. Norreys, A. P. Fews, F. N. Beg, A. R. Bell, A. E. Dangor, P. Lee, M. B. Nelson, H. Schmidt, M. Tatarakis, and M. D. Cable, Plasma Phys. Control. Fusion **40**, 175 (1998).
22. S. Karsch, S. Düsterer, H. Schwoerer, F. Ewald, D. Habs, M. Hegelich, G. Pretzler, A. Pukhov, K. Witte, and R. Sauerbrey, Phys. Rev. Lett. **91**, 015001 (2003).

23. S. Ter-Avetisyan, M. Schnürer, D. Hilscher, U. Jahnke, S. Busch, P. V. Nickles, and W. Sandner, Phys. Plasmas **12**, 2702 (2005).
24. K. L. Lancaster, S. Karsch, H. Habara, F. N. Beg, E. L. Clark, R. Freeman, M. H. Key, J. A. King, R. Kodama, K. Krushelnick, K. W. D. Ledingham, P. McKenna, C. D. Murphy, P. A. Norreys, R. Stephens, C. Stöeckl, Y. Toyama, M. S. Wei, and M. Zepf, Phys. Plasmas **11**, 3404 (2004).
25. M. Roth, D. Jung, K. Falk, N. Guler, O. Deppert, M. Devlin, A. Favalli, J. Fernandez, D. Gautier, M. Geissel, R. Haight, C. E. Hamilton, B. M. Hegelich, R. P. Johnson, F. Merrill, G. Schaumann, K. Schoenberg, M. Schollmeier, T. Shimada, T. Taddeucci, J. L. Tybo, F. Wagner, S. A. Wender, C. H. Wilde, and G. A. Wurden, Phys. Rev. Lett. **110**, 044802 (2013).
26. S. J. Gitomer, R. D. Jones, F. Begay, A. W. Ehler, J. F. Kephart, and R. Kristal, Phys. Fluids **29**, 2679 (1986).
27. D. Strickland and G. Morou, Opt. Commun. **56**, 219 (1985).
28. F. N. Beg, A. R. Bell, A. E. Dangor, C. N. Danson, A. P. Fews, M. E. Glinsky, B. A. Hammel, P. Lee, P. A. Norreys, and M. Tatarakis, Phys. Plasmas **4**, 447 (1997).
29. R. A. Snavely, M. H. Key, S. P. Hatchett, T. E. Cowan, M. Roth, T. W. Phillips, M. A. Stoyer, E. A. Henry, T. C. Sangster, M. S. Singh, S. C. Wilks, A. MacKinnon, A. Offenberger, D. M. Pennington, K. Yasuike, A. B. Langdon, B. F. Lasinski, J. Johnson, M. D. Perry, and E. M. Campbell, Phys. Rev. Lett. **85**, 2945 (2000).
30. S. C. Wilks, A. B. Langdon, T. E. Cowan, M. Roth, M. Singh, S. Hatchett, M. H. Key, D. Pennington, A. MacKinnon, and R. A. Snavely, Phys. Plasmas **8**, 542 (2001).
31. J. F. L. Simmons and C. R. McInnes, Amer. J. Phys. **61**, 205 (1993).
32. L. O. Silva, M. Marti, J. R. Davies, R. A. Fonseca, C. Ren, F. S. Tsung, and W. B. Mori, Phys. Rev. Lett. **92**, 015002 (2004).
33. W. Yu, H. Xu, F. He, M. Y. Yu, S. Ishiguro, J. Zhang, and A. Y. Wong, Phys. Rev. E **72**, 046401 (2005).
34. A. Macchi, F. Cattani, T. V. Liseykina, and F. Cornolti, Phys. Rev. Lett. **94**, 165003 (2005).
35. T. Esirkepov, M. Borghesi, S. V. Bulanov, G. Mourou, and T. Tajima, Phys. Rev. Lett. **92**, 175003 (2004).
36. X. Zhang, B. Shen, X. Li, Z. Jin, F. Wang, and M. Wen, Phys. Plasmas **14**, 123108 (2007).
37. A. Robinson, M. Zepf, S. Kar, R. Evans, and C. Bellei, New J. Phys. **10**, 013021 (2008).
38. O. Klimo, J. Psikal, J. Limpouch, and V. T. Tikhonchuk, Phys. Rev. ST Accel. Beams **11**, 031301 (2008).
39. X. Q. Yan, C. Lin, Z. M. Sheng, Z. Y. Guo, B. C. Liu, Y. R. Lu, J. X. Fang, and J. E. Chen, Phys. Rev. Lett. **100**, 135003 (2008).
40. B. Qiao, S. Kar, M. Geissler, P. Gibbon, M. Zepf, and M. Borghesi, Phys. Rev. Lett. **108**, 115002 (2012).
41. B. Shen and Z. Xu, Phys. Rev. E **64**, 056406 (2001).
42. B. Qiao, M. Zepf, M. Borghesi, and M. Geissler, Phys. Rev. Lett. **102**, 145002 (2009).
43. A. Macchi, S. Veghini, and F. Pegoraro, Phys. Rev. Lett. **103**, 085003 (2009).
44. B. Qiao, M. Zepf, P. Gibbon, M. Borghesi, J. Schreiber, and M. Geissler, Proc. SPIE **8079**, 80790Q (2011).
45. P. Lebedew, Ann. Phys. **311**, 433 (1901).
46. E. F. Nichols and G. F. Hull, Astrophys. J. **17**, 315 (1903).
47. F. A. Zander, Tech. Zhizn **13**, 15 (1924).
48. A. S. Eddington, Mon. Not. R. Astron. Soc. **85**, 408 (1925).
49. V. I. Veksler, Sov. J. At. Energy **2**, 525 (1957).
50. G. Marx, Nature **211**, 22 (1966).
51. A. Henig, S. Steinke, M. Schnürer, T. Sokollik, R. Hörlein, D. Kiefer, D. Jung, J. Schreiber, B. M. Hegelich, X. Q. Yan, J. Meyer-ter-Vehn, T. Tajima, P. V. Nickles, W. Sandner, and D. Habs, Phys. Rev. Lett. **103**, 245003 (2009).
52. M. Hegelich, S. Karsch, G. Pretzler, D. Habs, K. Witte, W. Guenther, M. Allen, A. Blazevic, J. Fuchs, J. C. Gauthier, M. Geissel, P. Audebert, T. Cowan, and M. Roth, Phys. Rev. Lett. **89**, 085002 (2002).
53. J. Schreiber, M. Kaluza, F. Grüner, U. Schramm, B. M. Hegelich, J. Cobble, M. Geissler, E. Brambrink, J. Fuchs, P. Audebert, D. Habs, and K. Witte, Appl. Phys. B **79**, 1041 (2004).
54. P. McKenna, F. Lindau, O. Lundh, D. C. Carroll, R. J. Clarke, K. W. D. Ledingham, T. McCanny, D. Neely, A. P. L. Robinson, L. Robson, P. T. Simpson, C.-G. Wahlström, and M. Zepf, Plasma Phys. Control. Fusion **49**, B223 (2007).
55. A. Henig, D. Kiefer, K. Markey, D. C. Gautier, K. A. Flippo, S. Letzring, R. P. Johnson, T. Shimada, L. Yin, B. J. Albright, K. J. Bowers, J. C. Fernández, S. G. Rykovanov, H.-C. Wu, M. Zepf, D. Jung, V. Kh. Liechtenstein, J. Schreiber, D. Habs, and B. M. Hegelich, Phys. Rev. Lett. **103**, 045002 (2009).
56. A. V. Brantov, V. T. Tikhonchuk, O. Klimo, D. V. Romanov, S. Ter-Avetisyan, M. Schnürer, T. Sokollik, and P. V. Nickles, Phys. Plasmas **13**, 122705 (2006).
57. J. Schreiber, F. Bell, F. Grüner, U. Schramm, M. Geissler, M. Schnürer, S. Ter-Avetisyan, B. M. Hegelich, J. Cobble, E. Brambrink, J. Fuchs, P. Audebert, and D. Habs, Phys. Rev. Lett. **97**, 045005 (2006).
58. J. Fuchs, P. Antici, E. d'Humières, E. Lefebvre, M. Borghesi, E. Brambrink, C. A. Cecchetti, M. Kaluza, V. Malka, M. Manclossi, S. Meyroneinc, P. Mora, J. Schreiber, T. Toncian, H. Pépin, and P. Audebert, AIP Conf. Proc. **827**, 237 (2006).
59. P. McKenna, K. W. D. Ledingham, J. M. Yang, L. Robson, T. McCanny, S. Shimizu, R. J. Clarke, D. Neely, K. Spohr, R. Chapman, R. P. Singhal, K. Krushelnick, M. S. Wei, and P. A. Norreys, Phys. Rev. E **70**, 036405 (2004).
60. Y. Murakami, Y. Kitagawa, Y. Sentoku, M. Mori, R. Kodama, K. A. Tanaka, K. Mima, and T. Yamanaka, Phys. Plasmas **8**, 4138 (2001).
61. S. Fritzler, V. Malka, G. Grillon, J.-P. Rousseau, F. Burgy, E. Lefebvre, E. dHumieres, P. McKenna, and K. W. D. Ledingham, Appl. Phys. Lett. **83**, 3039 (2003).
62. L. Robson, P. T. Simpson, R. J. Clarke, K. W. D. Ledingham, F. Lindau, O. Lundh, T. McCanny, P. Mora, D. Neely, C.-G. Wahlström, M. Zepf, and P. McKenna, Nat. Phys. **3**, 58 (2006).
63. M. Nishiuchi, A. Fukumi, H. Daido, Z. Li, A. Sagisaka, K. Ogura, S. Orimo, M. Kado, Y. Hayashi, M. Mori, S. V. Bulanov, T. Esirkepov, K. Nemoto, Y. Oishi, T. Nayuki, T. Fujii, A. Noda, Y. Iwashita, T. Shirai, and S. Nakamura, Phys. Lett. A **357**, 339 (2006).
64. E. L. Clark, K. Krushelnick, M. Zepf, F. N. Beg, M. Tatarakis, A. Machacek, M. I. K. Santala, I. Watts, P. A. Norreys, and A. E. Dangor, Phys. Rev. Lett. **85**, 1654 (2000).
65. T. Fujii, Y. Oishi, T. Nayuki, and Y. Takizawa, Appl. Phys. Lett. **83**, 1524 (2003).
66. I. Spencer, K. W. D. Ledingham, P. McKenna, T. McCanny, R. P. Singhal, P. S. Foster, D. Neely, A. J. Langley, E. J. Divall, C. J. Hooker, R. J. Clarke, P. A. Norreys, E. L. Clark, K. Krushelnick, and J. R. Davies, Phys. Rev. E **67**, 046402 (2003).
67. S. Kar, K. F. Kakolee, B. Qiao, A. Macchi, M. Cerchez, D. Doria, M. Geissler, P. McKenna, D. Neely, J. Osterholz, R. Prasad, K. Quinn, B. Ramakrishna, G. Sarri, O. Willi, X. Y. Yuan, M. Zepf, and M. Borghesi, Phys. Rev. Lett. **109**, 185006 (2012).
68. K. Ogura, M. Nishiuchi, A. S. Pirozhkov, T. Tanimoto, A. Sagisaka, T. Zh. Esirkepov, M. Kando, T. Shizuma,

T. Hayakawa, H. Kiriyama, T. Shimomura, S. Kondo, S. Kanazawa, Y. Nakai, H. Sasao, F. Sasao, Y. Fukuda, H. Sakaki, M. Kanasaki, A. Yogo, S. V. Bulanov, P. R. Bolton, and K. Kondo, Opt. Lett. **37**, 2868 (2012).
69. D. Jung, L. Yin, B. J. Albright, D. C. Gautier, S. Letzring, B. Dromey, M. Yeung, R. Hörlein, R. Shah, and S. Palaniyappan, New J. Phys. **15**, 023007 (2013).
70. D. Jung, L. Yin, D. C. Gautier, H.-C. Wu, S. Letzring, B. Dromey, R. Shah, S. Palaniyappan, T. Shimada, R. P. Johnson, J. Schreiber, D. Habs, J. C. Fernández, B. M. Hegelich, and B. J. Albright, Phys. Plasmas **20**, 083103 (2013).
71. A. Pukhov, Phys. Rev. Lett. **86**, 3562 (2001).
72. Q. L. Dong, Z. M. Sheng, M. Y. Yu, and J. Zhang, Phys. Rev. E **68**, 026408 (2003).
73. T. Esirkepov, M. Yamagiwa, and T. Tajima, Phys. Rev. Lett. **96**, 105001 (2006).
74. L. Yin, B. J. Albright, B. M. Hegelich, K. J. Bowers, K. A. Flippo, T. J. T. Kwan, and J. C. Fernández, Phys. Plasmas **14**, 056706 (2007).
75. X. Q. Yan, H. C. Wu, Z. M. Sheng, J. E. Chen, and J. Meyer-ter-Vehn, Phys. Rev. Lett. **103**, 135001 (2009).
76. J. Fuchs, P. Antici, E. d'Humières, E. Lefebvre, M. Borghesi, E. Brambrink, C. A. Cecchetti, M. Kaluza, V. Malka, M. Manclossi, S. Meyroneinc, P. Mora, J. Schreiber, T. Toncian, H. Pépin, and P. Audebert, Nat. Phys. **2**, 48 (2006).
77. M. Passoni and M. Lontano, Laser Part. Beams **22**, 163 (2004).
78. M. Lontano and M. Passoni, Phys. Plasmas **13**, 042102 (2006).
79. A. P. Robinson, A. R. Bell, and R. J. Kingham, Phys. Rev. Lett. **96**, 035005 (2006).
80. M. M. Basko, Eur. Phys. J. D **41**, 641 (2007).
81. M. Passoni and M. Lontano, Phys. Rev. Lett. **101**, 115001 (2008).
82. A. V. Brantov, V. T. Tikhonchuk, V. Y. Bychenkov, and S. G. Bochkarev, Phys. Plasmas **16**, 043107 (2009).
83. G. A. Mourou, T. Tajima, and S. V. Bulanov, Rev. Modern Phys. **78**, 309 (2006).
84. P. Mora, Phys. Rev. Lett. **90**, 185002 (2003).
85. S. S. Bulanov, V. Yu. Bychenkov, V. Chvykov, G. Kalinchenko, D. W. Litzenberg, T. Matsuoka, A. G. R. Thomas, L. Willingale, V. Yanovsky, K. Krushelnick, and A. Maksimchuk, Phys. Plasmas **17**, 043105 (2010).
86. J. Yu, Z. Jiang, J. C. Kieffer, and A. Krol, Phys. Plasmas **6**, 1318 (1999).
87. M. H. Key, M. D. Cable, T. E. Cowan, K. G. Estabrook, B. A. Hammel, S. P. Hatchett, E. A. Henry, D. E. Hinkel, J. D. Kilkenny, J. A. Koch, W. L. Kruer, A. B. Langdon, B. F. Lasinski, R. W. Lee, B. J. MacGowan, A. MacKinnon, J. D. Moody, M. J. Moran, A. A. Offenberger, D. M. Pennington, M. D. Perry, T. J. Phillips, T. C. Sangster, M. S. Singh, M. A. Stoyer, M. Tabak, G. L. Tietbohl, M. Tsukamoto, K. Wharton, and S. C. Wilks, Phys. Plasmas **5**, 1966 (1998).
88. L. D. Landau, J. S. Bell, M. J. Kearsley, L. P. Pitaevskii, E. M. Lifshitz, and J. B. Sykes, *Electrodynamics of Continuous Media*. Vol. 8 (Elsevier, 1984).
89. T. Toncian, M. Swantusch, M. Toncian, O. Willi, A. A. Andreev, and K. Y. Platonov, Phys. Plasmas **18**, 043105 (2011).
90. S. Steinke, P. Hilz, M. Schnürer, G. Priebe, J. Bränzel, F. Abicht, D. Kiefer, C. Kreuzer, T. Ostermayr, J. Schreiber, A. A. Andreev, T. P. Yu, A. Pukhov, and W. Sandner, Phys. Rev. ST Accel. Beams **16**, 011303 (2013).
91. J. Meyer-ter-Vehn and H.-C. Wu, Eur. Phys. J. D **55**, 433 (2009).
92. F. Pegoraro and S. V. Bulanov, Eur. Phys. J. D **55**, 399 (2009).
93. A. Andreev, A. Levy, T. Ceccotti, C. Thaury, K. Platonov, R. A. Loch, and P. Martin, Phys. Rev. Lett. **101**, 155002 (2008).
94. S. Steinke, A. Henig, M. Schnürer, T. Sokollik, P.V. Nickles, D. Jung, D. Kiefer, R. Hörlein, J. Schreiber, T. Tajima, X. Q. Yan, M. Hegelich, J. Meyer-ter-Vehn, W. Sandner, and D. Habs, Laser Part. Beams **28**, 215 (2010).
95. M. Chen, A. Pukhov, T. P. Yu, and Z. M. Sheng, Phys. Rev. Lett. **103**, 024801 (2009).
96. X. Q. Yan, T. Tajima, M. Hegelich, L. Yin, and D. Habs, Appl. Phys. B **98**, 711 (2010).
97. A. H. Sørensen, Phys. Rev. A **81**, 022901 (2010).
98. T. L. S. Group, CERN Report CERN-91-03 (1991).
99. H.-C. Wu, T. Tajima, D. Habs, A. W. Chao, and J. Meyer-ter-Vehn, Phys. Rev. ST Accel. Beams **13**, 101303 (2010).
100. A. Ferrari, G. R. Stevenson, and E. Weisse, in *Proceedings of 3rd European Particle Accelerator Conference* 1545 (1992).
101. S. V. Bulanov, T. Esirkepov, P. Migliozzi, F. Pegoraro, T. Tajima, and F. Terranova, Nucl. Instrum. Methods Phys. Res. A **540**, 25 (2005).
102. F. Pegoraro, S. V. Bulanov, J. I. Sakai, and G. Tomassini, Phys. Rev. E **64**, 016415 (2001).
103. S. V. Bulanov, E. Y. Echkina, T. Z. Esirkepov, I. N. Inovenkov, M. Kando, F. Pegoraro, and G. Korn, Phys. Plasmas **17**, 063102 (2010).
104. C. A. J. Palmer, T. Kluge, K. Zeil, M. Bussmann, S. D. Kraft, T. E. Cowan, and U. Schramm, Phys. Rev. Lett. **108**, 225002 (2012).
105. F. Pegoraro and S. V. Bulanov, Phys. Rev. Lett. **99**, 065002 (2007).
106. S. C. Wilks, W. L. Kruer, M. Tabak, and A. B. Langdon, Phys. Rev. Lett. **69**, 1383 (1992).
107. G. Mourou, Z. Chang, A. Maksimchuk, J. Nees, S. V. Bulanov, V. Yu. Bychenkov, T. Zh. Esirkepov, N. M. Naumova, F. Pegoraro, and H. Ruhl, Plasma Phys. Rep. **28**, 12 (2002).
108. A. J. Mackinnon, Y. Sentoku, P. K. Patel, D. W. Price, S. Hatchett, M. H. Key, C. Andersen, R. Snavely, and R. R. Freeman, Phys. Rev. Lett. **88**, 215006 (2002).
109. B. Shen, X. Zhang, Z. Sheng, M. Y. Yu, and J. Cary, Phys. Rev. ST Accel. Beams **12**, 121301 (2009).
110. X. Zhang, B. Shen, L. Ji, F. Wang, M. Wen, W. Wang, J. Xu, and Y. Yu, Phys. Plasmas **17**, 123102 (2010).
111. F. L. Zheng, S. Z. Wu, H. C. Wu, C. T. Zhou, H. B. Cai, M. Y. Yu, T. Tajima, X. Q. Yan, and X. T. He, Phys. Plasmas **20**, 013107 (2013).
112. J. H. Bin, W. J. Ma, K. Allinger, H. Y. Wang, D. Kiefer, S. Reinhardt, P. Hilz, K. Khrennikov, S. Karsch, X. Yan, F. Krausz, T. Tajima, D. Habs, and J. Schreiber, Phys. Plasmas **20**, 073113 (2013).
113. K. Zeil, S. D. Kraft, S. Bock, M. Bussmann, T. E. Cowan, T. Kluge, J. Metzkes, T. Richter, R. Sauerbrey, and U. Schramm, New J. Phys. **12**, 045015 (2010).
114. I. J. Kim, K. H. Pae, C. M. Kim, H. T. Kim, J. H. Sung, S. K. Lee, T. J. Yu, I. W. Choi, C.-L. Lee, K. H. Nam, P. V. Nickles, T. M. Jeong, and J. Lee, Phys. Rev. Lett. **111**, 165003 (2013).
115. J. S. Green, A. P. L. Robinson, N. Booth, D. C. Carroll, R. J. Dance, R. J. Gray, D. A. MacLellan, P. McKenna, C. D. Murphy, D. Rusby, and L. Wilson, Appl. Phys. Lett. **104**, 214101 (2014).
116. D. Jung, *Ion acceleration from relativistic laser nano-target interaction* Dissertation (LMU München, 2012).
117. H. Y. Wang, C. Lin, F. L. Zheng, Y. R. Lu, Z. Y. Guo, X. T. He, J. E. Chen, and X. Q. Yan, Phys. Plasmas **18**, 093105 (2011).
118. A. Sgattoni, S. Sinigardi, and A. Macchi, Appl. Phys. Lett. **105**, 084105 (2014).